

Molecule–Electrode Bonding Design for High Single-Molecule Conductance

Kazumichi Yokota,[†] Masateru Taniguchi,^{*,†,‡} Makusu Tsutsui,[†] and Tomoji Kawai^{*,†}

The Institute of Scientific and Industrial Research, Osaka University, 8-1 Ibaraki, Osaka 567-0047, Japan, and PRESTO, Japan Science and Technology Agency, Honcho, Kawaguchi, Saitama 332-0012, Japan

Received September 6, 2010; E-mail: taniguti@sanken.osaka-u.ac.jp; kawai@sanken.osaka-u.ac.jp

Abstract: We report the application of an intermolecular interaction design for organic conductor crystals with a high conductance to a molecule–electrode design for a high single-molecule conductance by using dithiol and diselenol terthiophenes. We found that dithiol and diselenol single-molecule junctions show the highest single-molecule conductance among single-molecule junctions with Au–S and Au–Se bonds, and that diselenol single-molecule junctions have a higher single-molecule conductance than dithiol ones. We demonstrate that replacing S atoms with Se atoms is a promising molecule–electrode bonding design for a high single-molecule conductance.

Major challenges that exist in the development of single-molecule devices lie in creating electronic devices and controlling their characteristics when they are cut off from intermolecular interactions, although many properties of the materials stem from such interactions. The only intermolecular interaction in single-molecule devices is a molecule–electrode bond, which dominates the electrical properties.¹ Substitution of large heteroatoms in molecules is a sophisticated intermolecular interaction design for obtaining a high electrical conductance in organic conductor crystals; a high conductance can be obtained by replacing S atoms in molecules with Se atoms.² We anticipate that the intermolecular interaction design of organic conductor crystals can be applied to the molecule–electrode bonding design of single-molecule devices, although the guiding principles for obtaining the high single-molecule conductance desirable for stable device operation are still unclear. This study addresses the issue using terthiophenedithiol (3TS) and terthiophenediselenol (3TSe).

Terthiophenes were selected as candidates likely to have a high single-molecule conductance because of their small highest occupied molecular orbital–lowest unoccupied molecular orbital (HOMO–LUMO) gaps. 3TS and 3TSe were obtained from corresponding bis(acetylthio)- and bis(acetylseleno)terthiophenes.³ Conductance traces were measured at room temperature and 0.2 V under vacuum using nanofabricated mechanically controllable break junctions.⁴ Both typical conductance traces showed conductance plateaus at $1G_0$ ($G_0 = 77.5 \mu\text{S}$) corresponding to the formation of single-Au atomic contacts (Figure 1a and 1b).⁵ In the 3TS conductance traces, conductance plateaus were observed around $0.1G_0$ after the observation of a conductance plateau around $1.1G_0$. Conductance plateaus were also observed sequentially around $1.2G_0$, $0.2G_0$, and $0.1G_0$. The 3TSe conductance traces showed plateaus around $0.15G_0$ after $1.15G_0$ and at $0.3G_0$ after $1.3G_0$. Conductance histograms for 3TS and 3TSe junctions were constructed without data selection from 1000 and 1100 conductance traces, respectively (Figure 1c

and 1d). The conductance histograms for 3TS and 3TSe junctions show pronounced peaks at integer multiples of $0.12G_0$ and $0.16G_0$, respectively. Therefore, the single-molecule conductances of 3TS and 3TSe were determined to be $G_{3\text{TS}} = 0.12G_0$ ⁶ and $G_{3\text{TSe}} = 0.16G_0$, respectively. We found that both molecule junctions show the highest single-molecule conductance among single-molecule junctions having S–Au and Se–Au bonds.^{1b,d}

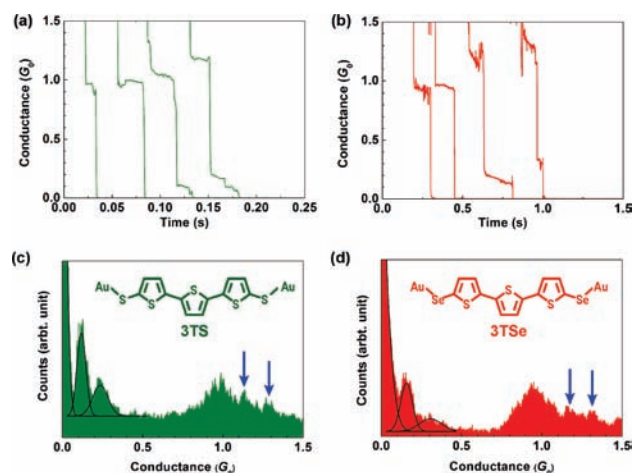


Figure 1. Conductance characteristics of 3TS and 3TSe junctions. Au electrodes were used. Typical conductance traces of (a) 3TS and (b) 3TSe junctions. Conductance histograms of (c) 3TS and (d) 3TSe junctions constructed from 1000 and 1100 conductance traces, respectively. Black lines show Gaussian fitting to peak profiles. Conductance peaks in (c) and (d) are observed at integer multiples of $G_{3\text{TS}} = 0.12G_0$ and $G_{3\text{TSe}} = 0.16G_0$, corresponding to the 3TS and 3TSe single-molecule conductance, respectively. Conductance peaks at $G_{\text{Au}} = 1G_0$ correspond to the formation of single-Au atomic contacts. Blue arrows show conductance peaks at $1.12G_0$ ($G_{\text{Au}} + G_{3\text{TS}}$), $1.24G_0$ ($G_{\text{Au}} + 2G_{3\text{TS}}$), $1.16G_0$ ($G_{\text{Au}} + G_{3\text{TSe}}$), and $1.31G_0$ ($G_{\text{Au}} + 2G_{3\text{TSe}}$), indicating that single- and double-molecule junctions formed parallel to single-Au atomic contacts.

The single-molecule conductance depends on the HOMO–LUMO gaps, energy level alignment between molecules and electrodes, and molecule–electrode coupling strength.^{1a–c} The calculated HOMO–LUMO gap (3.2 eV) of 3TS is the same as that of 3TSe.⁷ The degree of charge transfer from molecule to electrodes is the same in 3TS and 3TSe single-molecule junctions, since the calculated HOMO energy level (–4.5 eV) is the same in 3TS and 3TSe. As a result, the energy level alignment between molecules and electrodes is the same in 3TS and 3TSe single-molecule junctions. Therefore, the difference in 3TS and 3TSe single-molecule conductances is expected to originate from the molecule–electrode coupling strength. When molecules are bonded to electrodes via S–Au and Se–Au bonds, π bonds are formed by the 6s orbitals of Au and the p_z orbitals of S and Se. The transfer integrals of Se–Au bonds (114 meV) are larger than those of S–Au bonds (107 meV).⁸ The molecule–electrode coupling strength of

[†] The Institute of Scientific and Industrial Research, Osaka University.

[‡] PRESTO, Japan Science and Technology Agency.

Se–Au bonds is stronger than that of S–Au bonds for π bonding, because the molecule–electrode coupling strength increases with increasing transfer integral.^{1a–c,9} Since the single-molecule conductance increases as the molecule–electrode coupling strength increases, single-molecule junctions with Se–Au bonds have a higher single-molecule conductance than those with S–Au bonds.^{7,10} Such an achievement of a higher single-molecule conductance by replacement of S with Se atoms has been predicted theoretically.¹¹ However, over the course of single-molecule-device development, the phenomenon has not heretofore been demonstrated. We have now confirmed the theoretical prediction, thus, improving the electric-conduction properties of current molecular devices.

In sharp contrast to the present results, we have demonstrated that single-molecule junctions with Se–Au bonds have a lower single-molecule conductance than those with S–Au bonds when σ bonds form between S–Au and Se–Au.¹² Although the molecule–electrode coupling strength of Se–Au bonds is stronger than that of S–Au bonds for σ bonding, σ bonds certainly lead to very strong molecule–electrode coupling. Since overly strong molecule–electrode coupling localizes mobile electrons at molecule–electrode bonds, single-molecule conductance decreases as the molecule–electrode coupling strength increases.^{1a} Therefore, although replacing S atoms with Se atoms is a molecule–electrode bonding design suitable for a high single-molecule conductance, the molecule–electrode bonding type must be simultaneously designed to obtain a high single-molecule conductance. Thus, intermolecular interaction design for controlling conductance in organic conductor crystals is applicable to molecule–electrode design for controlling single-molecule conductance, even though only molecule–electrode interactions can be controlled at single-molecule junctions.

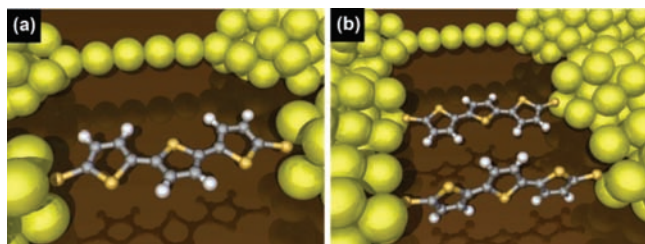


Figure 2. Schematic illustrations of high conductance states suggested by conductance histograms. (a) High conductance peaks of $1.12G_0$ ($G_{\text{Au}} + G_{3\text{TSe}}$) and $1.16G_0$ ($G_{\text{Au}} + G_{3\text{TSe}}$) show that single-molecule junctions formed parallel to single-Au atomic contacts, whereas (b) those of $1.24G_0$ ($G_{\text{Au}} + 2G_{3\text{TSe}}$) and $1.31G_0$ ($G_{\text{Au}} + 2G_{3\text{TSe}}$) show the formation of multiple double-molecule junctions and single-Au atomic junctions.

We intuitively expect that multiple junctions can be formed by single-Au atomic contacts and single- or double-molecule junctions, since the length of single-Au atomic contacts is similar to that of single- and double-molecule junctions. However, the formation of multiple junctions is unprecedented.¹³ As clearly shown in Figure 1c and 1d, pronounced conductance peaks were observed at $1.12G_0$ and $1.24G_0$ in the conductance histogram for 3TS junctions and at $1.16G_0$ and $1.31G_0$ in that for 3TSe junctions. Conductances of $1.12G_0$ and $1.24G_0$ are composed of $G_{\text{Au}} + G_{3\text{TSe}}$ and $G_{\text{Au}} + 2G_{3\text{TSe}}$, respectively, and those of $1.16G_0$ and $1.31G_0$ are composed of $G_{\text{Au}} + G_{3\text{TSe}}$ and $G_{\text{Au}} + 2G_{3\text{TSe}}$, respectively. The conductance peaks at more than $1G_0$ clearly demonstrate that single- and double-molecule junctions formed parallel to single-Au atomic contacts (Figure 2). The conductance peaks corresponding to the formation of multiple junctions provide information about the formation mechanism:

single-molecule junctions form after multiple single-Au atomic contacts and single-molecule junctions are formed and single-Au atomic contacts are fractured. Observation of high conductance peaks for multiple single-Au atomic contacts and molecular junctions can be realized only by obtaining a high single-molecule conductance, which strongly supports the claim that conductances of $0.12G_0$ and $0.16G_0$ correspond to the single-molecule conductances of 3TS and 3TSe, respectively.

In summary, this study demonstrates that 3TS and 3TSe single-molecule junctions have high single-molecule conductances of more than $0.1G_0$ and that the single-molecule conductance of 3TSe junctions is higher than that of 3TS junctions. This high single-molecule conductance enabled the first observation of multiple junctions in which single-molecule junctions formed parallel to single-Au atomic contacts. We demonstrate that intermolecular interaction design for obtaining a high conductance in organic conductor crystals is applicable to the molecule–electrode bonding design for high single-molecule conductance. Since intermolecular interaction design for forming two-dimensional intermolecular interactions for high conductance in organic conductor crystals² can be interpreted as the formation of single-molecule junctions via multiple molecule–electrode bonds, single-molecule junctions with multiple bonding sites are expected to have a high single-molecule conductance.

Acknowledgment. This research is partially supported by the Japan Society for the Promotion of Science (JSPS) through its Funding Program for World-Leading Innovative R&D on Science and Technology.

Supporting Information Available: Sample preparation and theoretical calculations. This material is available free of charge via the Internet at <http://pubs.acs.org>.

References

- (1) (a) Datta, S. *Electric Transport in Mesoscopic Systems*; Cambridge University Press: Cambridge, 1995. (b) Linsay, S. M.; Ratner, M. A. *Adv. Mater.* **2007**, *19*, 23–31. (c) Nitzan, A.; Ratner, M. A. *Science* **2003**, *300*, 1384–1389. (d) Tao, N. J. *Nat. Nanotechnol.* **2006**, *1*, 173–181.
- (2) (a) Williams, J. M.; Ferraro, J. R.; Thorn, R. J.; Carlson, K. D.; Geiser, U.; Wang, H. H. *Organic Superconductors*; Prentice Hall: NJ, 1992. (b) Saito, G.; Kagoshima, S. *The Physics and Chemistry of Organic Superconductors*; Springer-Verlag: Heidelberg, 1990.
- (3) (a) de Boer, B.; Meng, H.; Perepichka, D. F.; Zheng, J.; Frank, M. M.; Chabal, Y. J.; Bao, Z. *Langmuir* **2003**, *19*, 4272–4284. (b) Taniguchi, S.; Minamoto, M.; Matsushita, M. M.; Sugawara, T.; Kawada, Y.; Bethell, D. *J. Mater. Chem.* **2006**, *16*, 3459–3465.
- (4) (a) van Ruitenbeek, J. M.; Joyez, P.; Devoret, M. H.; Esteve, D.; Urbina, C. *Rev. Sci. Instrum.* **1996**, *67*, 108–111. (b) Tsutsui, M.; Shoji, K.; Taniguchi, M.; Kawai, T. *Nano Lett.* **2008**, *8*, 3293–3297.
- (5) Agrait, N.; Yeyati, A. L.; van Ruitenbeek, J. M. *Phys. Rep.* **2003**, *377*, 81–279.
- (6) Dulić, D.; Pump, F.; Campidelli, S.; Lavie, P.; Cuniberti, G.; Filoramo, A. *Angew. Chem., Int. Ed.* **2009**, *48*, 8273–8276.
- (7) Patrone, L.; Palacin, S.; Charlier, J.; Armand, F.; Bourgoin, J. P.; Tang, H.; Gauthier, S. *Phys. Rev. Lett.* **2003**, *91*, 096802–096805.
- (8) Transfer integrals were calculated using Au–3TS–Au and Au–3TSe–Au junctions as described in the Supporting Information.
- (9) Tada, T.; Yoshizawa, K. *ChemPhysChem* **2002**, *3*, 1035–1037.
- (10) (a) Patrone, L.; Palacin, S.; Bourgoin, J. P.; Lagoute, J.; Zambelli, T.; Gauthier, S. *Chem. Phys.* **2002**, *281*, 325–331. (b) Patrone, L.; Palacin, S.; Bourgoin, J. P. *Appl. Surf. Sci.* **2003**, *212–213*, 446–451. (c) Yokota, K.; Taniguchi, M.; Kawai, T. *J. Phys. Chem.* **2010**, *114*, 4044–4050.
- (11) Di Ventra, M.; Lang, N. D. *Phys. Rev. B* **2002**, *65*, 045402–045409.
- (12) Taniguchi, M.; Tsutsui, M.; Shoji, K.; Fujiwara, H.; Kawai, T. *J. Am. Chem. Soc.* **2009**, *131*, 14146–1414.
- (13) (a) Jian, W. B.; Chang, C. S.; Li, W. Y.; Tsong, Tien T. *Phys. Rev. B* **1999**, *59*, 3168–3172. (b) Yanson, I. K.; Shklyarevskii, O. I.; Csonka, Sz.; van Kempen, H.; Speller, S.; Yanson, A. I.; van Ruitenbeek, J. M. *Phys. Rev. Lett.* **2005**, *95*, 256806–256809.

JA108032Q